# Supporting Information

# Monodisperse Pattern Nanoalloying for Synergistic Intermetallic Catalysis

*Jeong Ho Mun[1,2], Yun Hee Chang[1,3], Dong Ok Shin[4], Jong Moon Yoon[1,2], Dong Sung Choi[1,2], Kyung-Min Lee[5], Ju Young Kim[1,2], Seung Keun Cha[1,2], Jeong Yong Lee[1,2], Jong-Ryul Jeong[5], Yong-Hyun Kim[1,3*] and Sang Ouk Kim[1,2*]*

[1]Center for Nanomaterials and Chemical Reactions, Institute for Basic Science (IBS), Daejeon 305-701, Republic of Korea.

[2]Department of Materials Science and Engineering, KAIST, Daejeon 305-701, Republic of Korea.

[3]Graduate School of Nanoscience and Technology, KAIST, Daejeon 305-701, Republic of Korea

[4]Power Control Device Research Section, Electronics and Telecommunications Researh Institute (ETRI), Daejeon 305-700, Republic of Korea

[5]Department of Materials Science and Engineering and Graduate School of Green Energy Technology, Chungnam National University, Daejeon 305-764, Republic of Korea

* To whom correspondence should be addressed. E-mail: sangouk.kim@kaist.ac.kr, yong.hyun.kim@kaist.ac.kr

Phone numbers to Sang Ouk Kim

Office phone: +82-42-350-3339

## Methods

**Preparation of BCP thin film templates:** Thin films of PS-*b*-P4VPs (Mn : 24000 & 48000 g/mol for PS and 9500 & 20500 g/mol for P4VP, purchased from Polymer Source Inc.) were spin-casted from 0.5 wt% solution in toluene/THF = 3/1 (weight ratio) onto an UV-Ozone treated substrates, including silicon, silica, glass, ITO, zirconia, zinc oxide (sol-gel method) and titania (atomic layer deposition). After deposition, BCP thin films were annealed under the saturated vapor evaporated from 2/8 (vol. ratio) toluene/THF = 2/8 mixture solvent for 6 hrs at room temperature for self-assembly.

**Fabrication of multimetallic nanoalloy array:** Multiple metallic complex anions were loaded into P4VP cylindrical nanodomains by immersing BCP templates into 3% HCl aqueous solution. After predetermined precursor loading time, BCP template was recovered and thoroughly rinsed with deionized water. Oxygen plasma treatment (40 sccm $O_2$ & 50 W) over the entire BCP thin area for 1 minute completely removed nonmetallic elements and remained multimetallic nanoclusters at the substrate surface. Subsequent thermal calcination under $Ar/H_2$ atmospheres at 400-650 °C (650 °C for FePt, FeCo, CoPt & CoPdPt, 400 °C for AuPd) for 30 min agglomerated and crystallized nanoclusters to form intermetallic nanoalloy array.

**Preparation for TEM samples:** Nanoalloy arrays fabricated on the silicon substrate was used for TEM sample preparation. Carbon deposition was done for the sample protection during sample processing. After polishing out the backside of the substrate, nanoalloys remaining on the sufficiently thinned silicon films were transferred to copper grids (GA2000-Cu, 2 mm aperture). Subsequent ion-milling was done until the sample thickness became 2-3 μm.

**Catalytic vertical CNT growth by PECVD:** Vertical CNT forests were grown from Fe-Co nanoalloy arrays prepared on silica substrates by catalytic PECVD. The alloy arrays were annealed at 700 °C under the stream of a $H_2/NH_3$ (80 sccm/20 sccm) gas mixture for 2 min for thermal reduction. Afterwards, the

chamber pressure was adjusted to 4 Torr. Application of 500 V DC power generated plasma environment. Slow streaming of the acetylene gas resulted in the growth of vertical CNT arrays.

**Characterization:** Nanoscale morphology of BCP thin films, metal nanoalloy arrays and the vertical CNT arrays were imaged using a Hitachi S-4800 FE-SEM. Atomic crystalline structure characterization, statistical dimension analysis and elemental mapping of intermetallic alloys were performed with a Cs-corrected JEM-ARM200F HR-TEM. For elemental mapping, the acquisition time was 30 min for Fe-Pt and 20 min for other alloys. The intermatallic phases of Fe-Pt nanoalloys were also characterized by X-ray diffraction (RIGAKU, D/MAX-2500) with Cu Kα radiation.

**DFT Theoretical calculation** DFT calculations were performed for bulk and (110) surfaces of Fe and FeCo alloys with the Vienna Ab Initio Simulation package (VASP)[1]. Kohn-Sham wave functions were expanded by a series of plane waves with a kinetic energy cutoff of 400 eV. The projected augmented wave (PAW) potentials[2] and the exchange-correlation functional of the Perdew-Berke-Ernzerhof (PBE)[3] were used to calculate electron-ion and electron-electron interactions, respectively. 128 atoms (0.78 % C) and 16 atoms (6.25 % C) FeCo supercells were used for calculating bulk properties. FeCo (110) slab model with the p(3×4) surface unit cell (24 surface Co and Fe atoms) and six atomic layers were used for calculating surface properties. For simplicity, body-centered cubic (bcc) structure was employed for Fe and Fe-Co alloy. It is noteworthy that the experimental CNT growth temperature (973K) is lower than the nanoparticle melting temperature predicted by liquid drop model[4]. The calculated formation energy and diffusion barrier of interstitial C in bulk Fe are well consistent with the experimental values, i.e., 0.74 eV for the formation energy and 0.86 eV for the diffusion barrier.

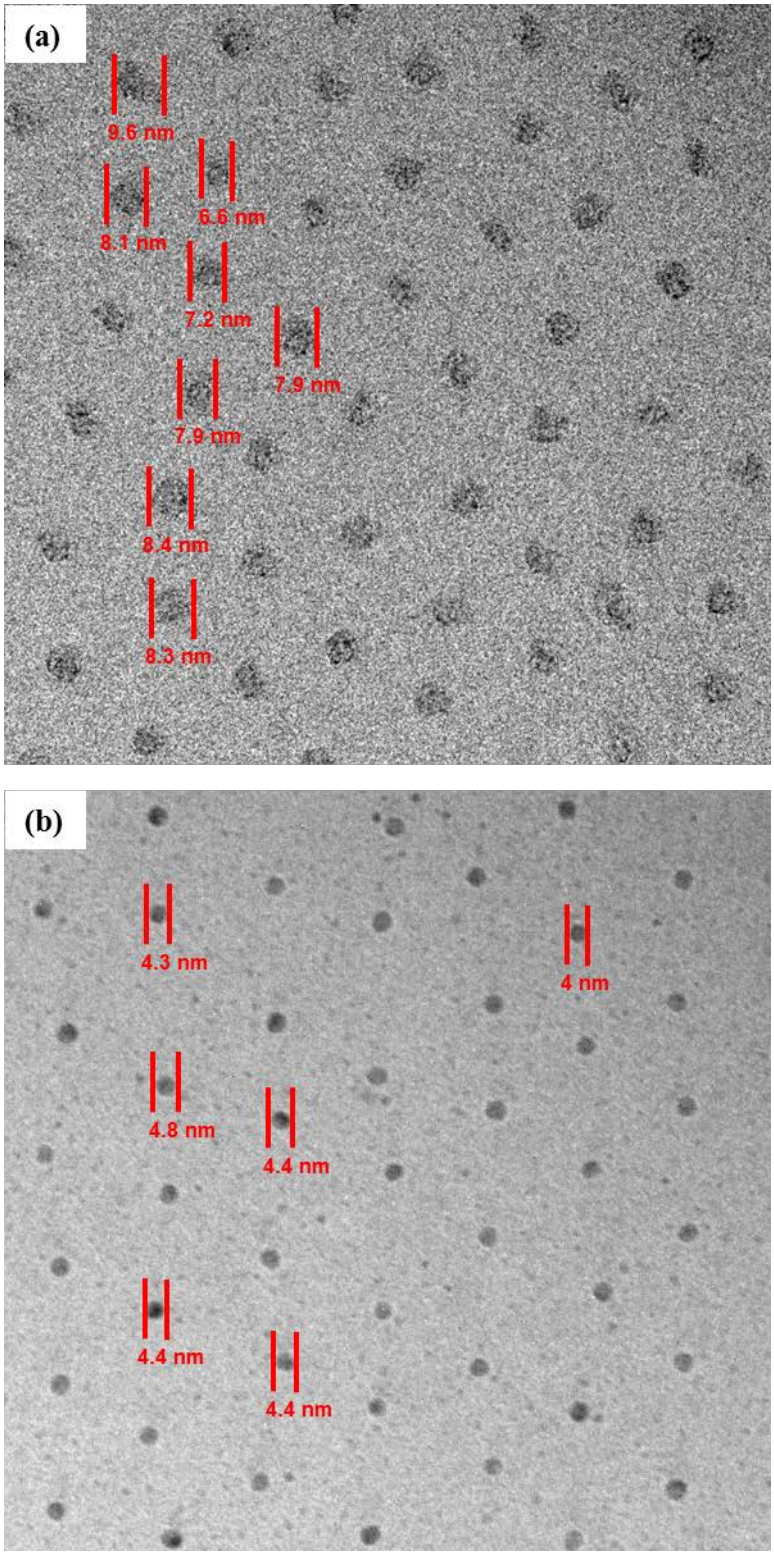


**Figure S1.** TEM images for statistical size distribution of (a) nanocluster and (b) nanoalloy arrays. The mean diameter and standard deviation were obtained from more than 200 clusters or particles employing the TEM image analysis tool implemented with DigitalMicrograph (TM) (Gatan Inc. Ver. 3.6.1).

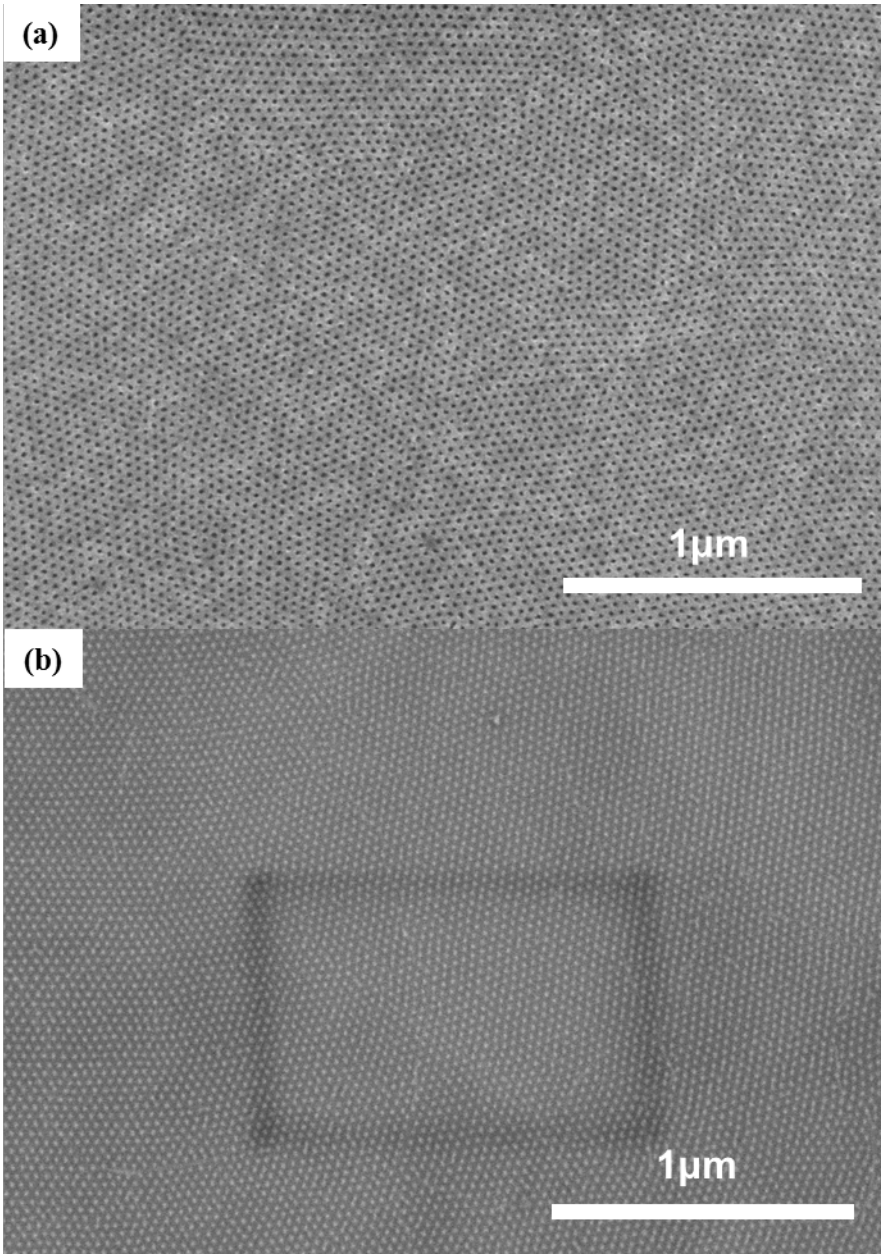


**Figure S2.** SEM images of (a) annealed BCP thin film and (b) resultant alloy array in a large area silicon substrate.

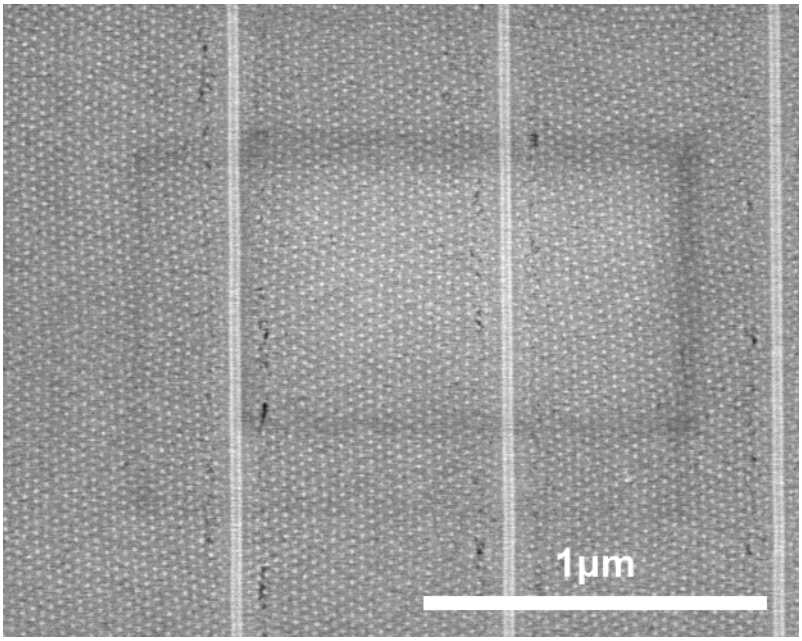


**Figure S3.** SEM image of graphoepitaxially aligned alloy nanodot array in zirconia trench.

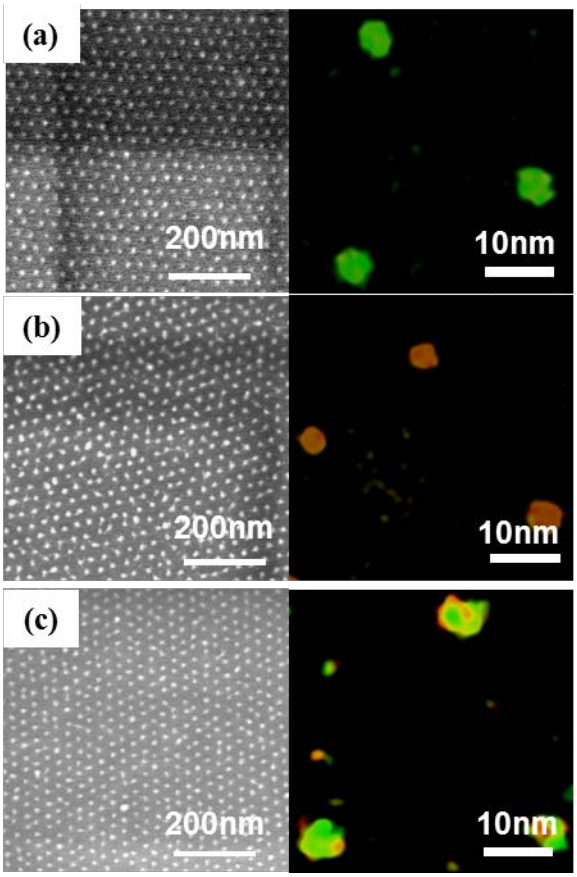


**Figure S4.** SEM and elemental mapping images of single-crystalline (a) Pt-Co, (b) Pd-Au binary alloy and (c) Co-Pd-Pt ternary alloy arrays.

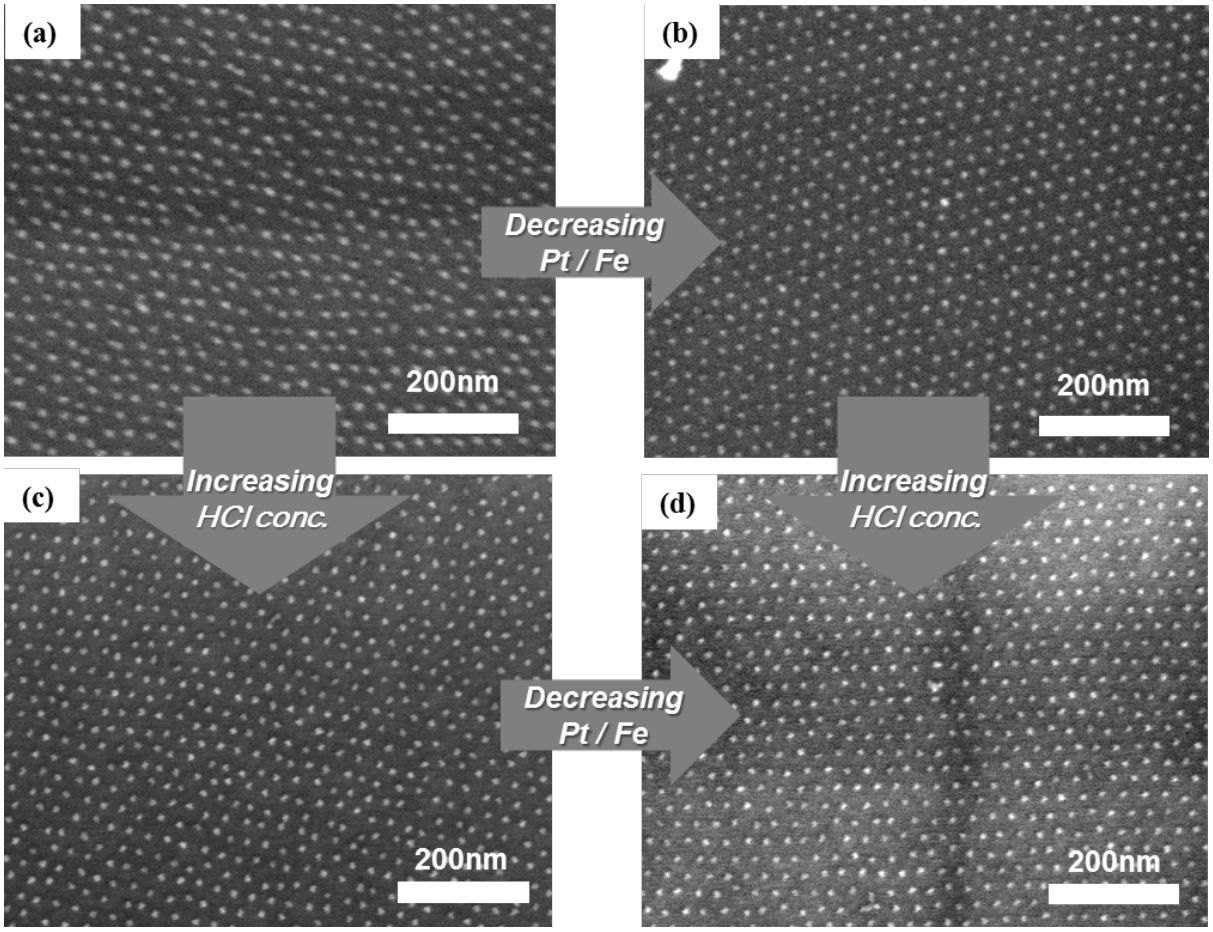


**Figure S5**. SEM images of Fe-Pt array loaded in different acidic conditions. (a) $K_3[Fe(CN)_6]$: $Na_2[PtCl_4]$ = 0.2 mM:0.8 mM with 0.1% HCl. (b) $K_3[Fe(CN)_{6]}$:$Na_2[PtCl_4]$ = 0.4 mM:0.6 mM with 0.1% HCl. (c) $K_3[Fe(CN)_6]$:$Na_2[PtCl_4]$ = 0.2 mM:0.8 mM with 3% HCl. (d) $K_3[Fe(CN_)_6]$:$Na_2[PtCl_4]$ = 0.4 mM:0.6 mM with 3% HCl.

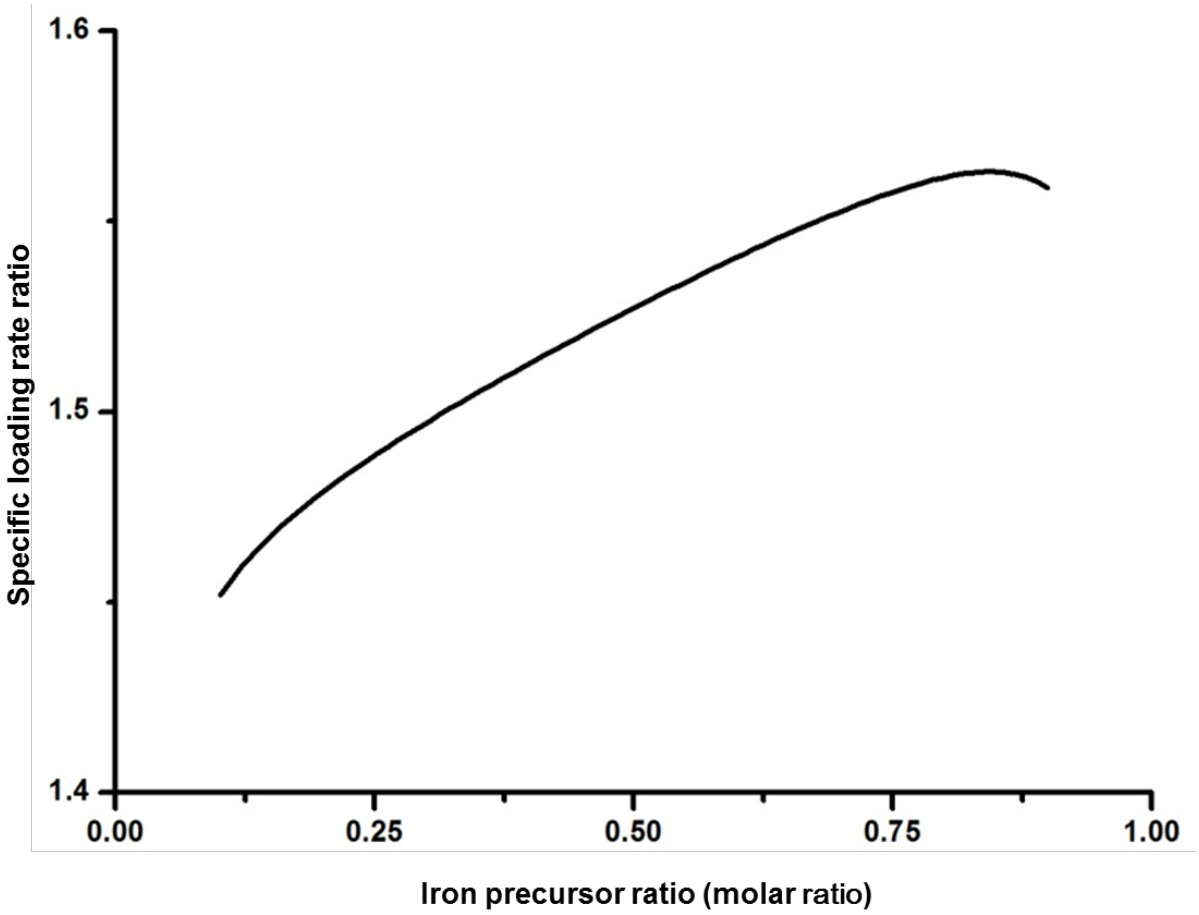


**Figure S6.** Specific loading rate ratio of Fe over Pt precursor. The loading ratio is maintained around 1.5 over entire precursor composition in the precursor solution.

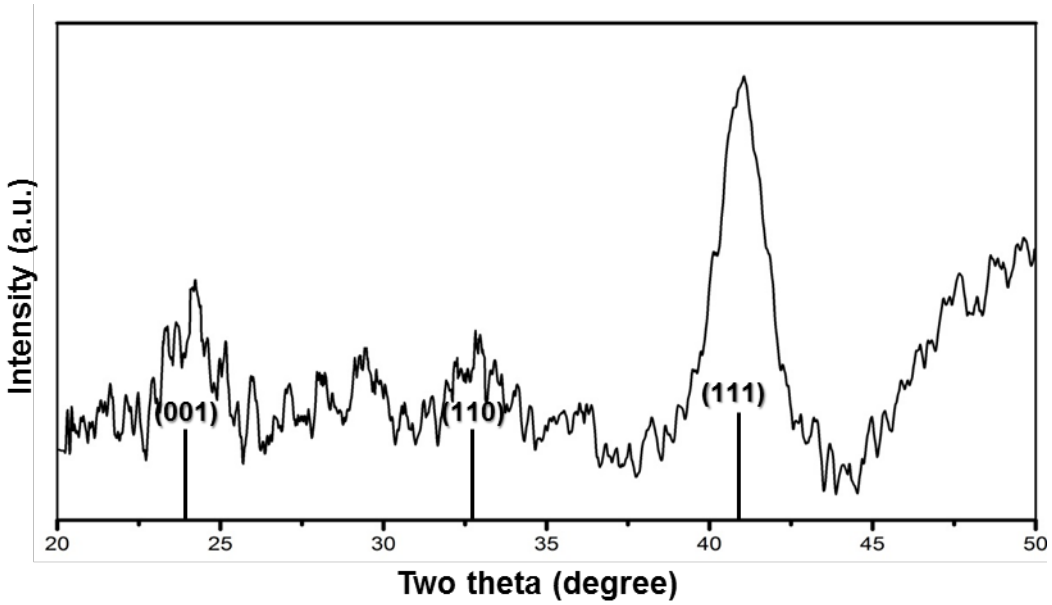


**Figure S7.** XRD of FePt alloy array. The atomic composition was ~1:1. The sample was thermally annealed at 650 °C under a hydrogen and argon atmosphere for 30 min. The diffraction pattern indicates FePt FCT phase.

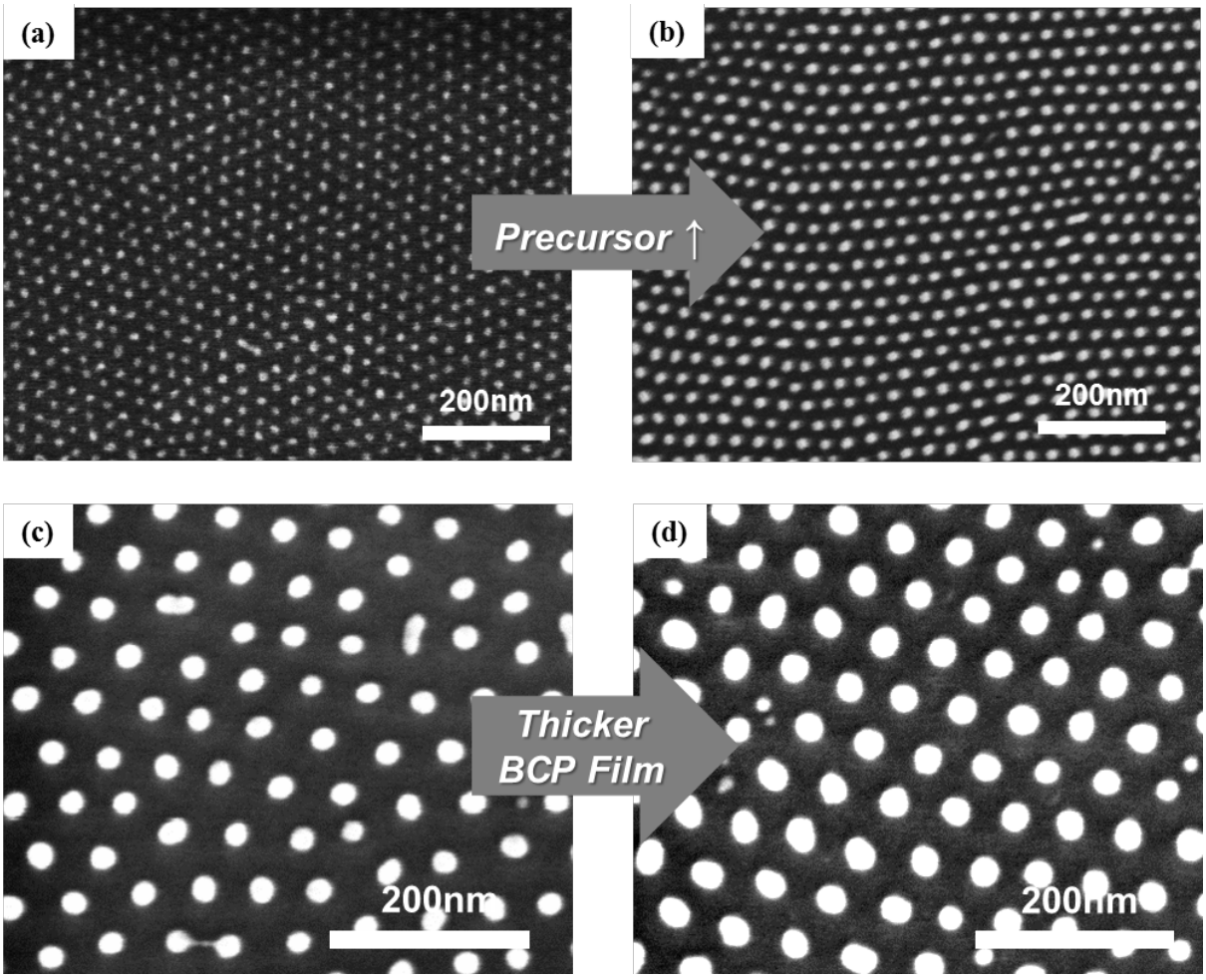


**Figure S8.** SEM images of Fe-Pt array. 3% HCl aqueous solution were employed. Alloy cluster size is tunable in a wide range, as shown in (a) average diameter of ~ 12 nm with $K_3[Fe(CN)_6]$:$Na_2[PtCl_4]$ = 0.4 mM:0.6 mM and (b) average diameter of ~ 17 nm with $K_3[Fe(CN)_6]$:$Na_2[PtCl_4]$ = 1.2 mM:1.8 mM. PS(24,000 g/mol)-*b*-P4VP(9,500 g/mol) templates was used for (a) and (b). (c) Average diameter of ~ 25nm was prepared from BCP film thickness of 30 nm. (d) Average diameter of ~ 30 nm was prepared from BCP film thickness ~ 40 nm. PS(48,000 g/mol)-*b*-P4VP(20,500 g/mol) templates and $K_3[Fe(CN)_6]$:$Na_2[PtCl_4]$ = 0.4 mM:0.6 mM were used for (c) and (d).

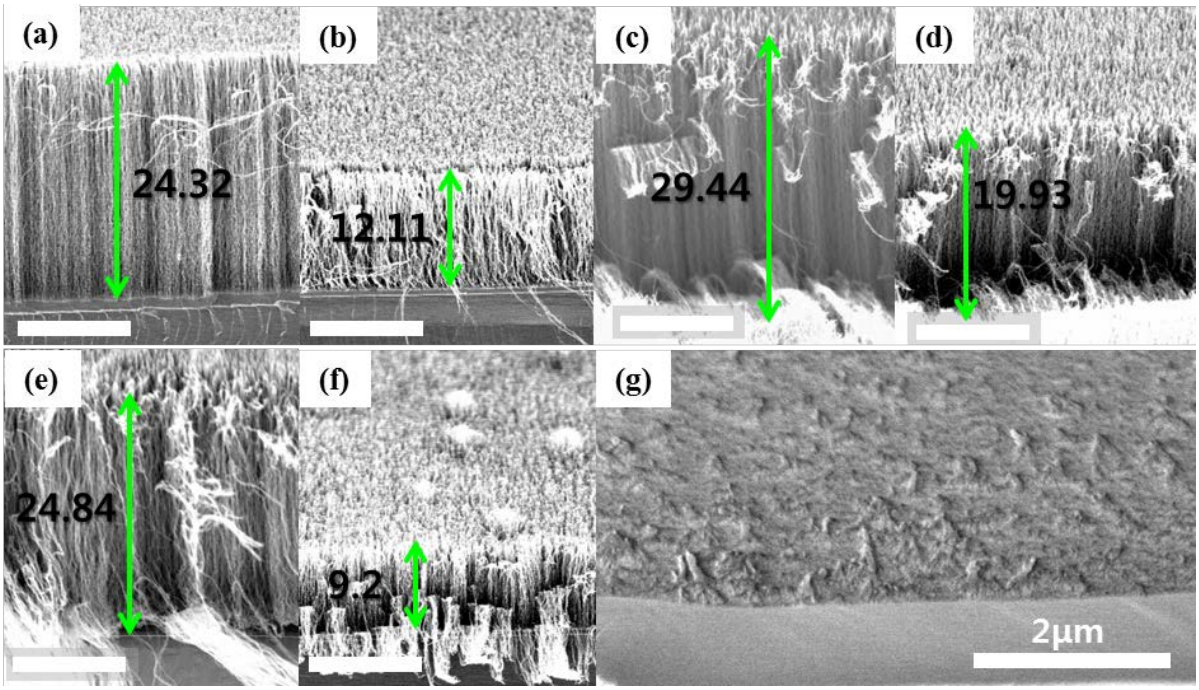


**Figure S9.** Tilted SEM images of vertical CNTs grown from Fe-Co alloy nanocatalyst arrays prepared with the metal precursor loading times of (a) & (b) for 3 min, (c) & (d) for 5 min and (e) & (f) for 9 min, respectively. The precursor molar ratios were split into (a), (c), and (e) for Fe/Co = 4/6 and (b), (d) and (f) for Fe/Co = 2/8. Each scale bar is 10 μm. (g) Barely grown CNTs from pure Co nanocatalyst array.

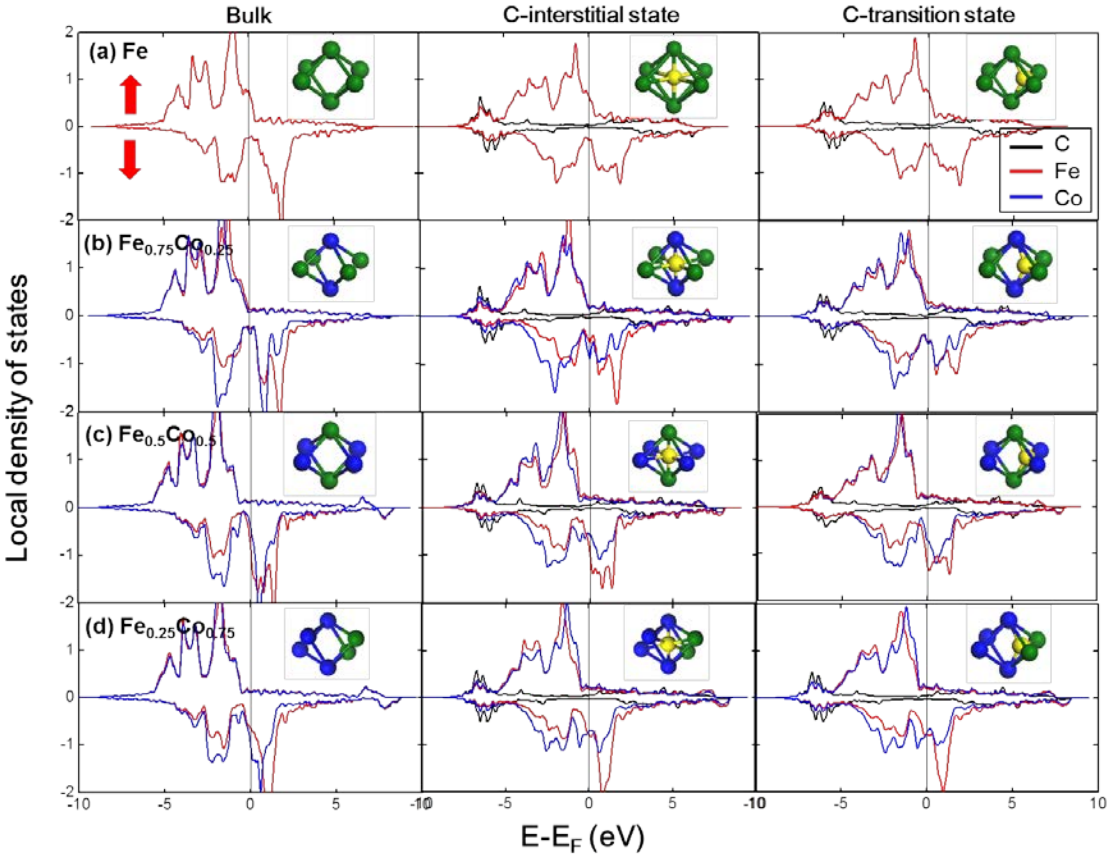


**Figure S10.** Calculated partial density of states of bulk, C-interstitial and C-transition state in (a) Fe, (b) $Fe_1Co_3$, (c) FeCo, and (d) $Fe_3Co_1$ . Black, red, and blue lines indicate the C, Fe, and Co, respectively. The up and down arrows indicate the majority and minority spins. Insets show the atomic structures at various diffusional states.

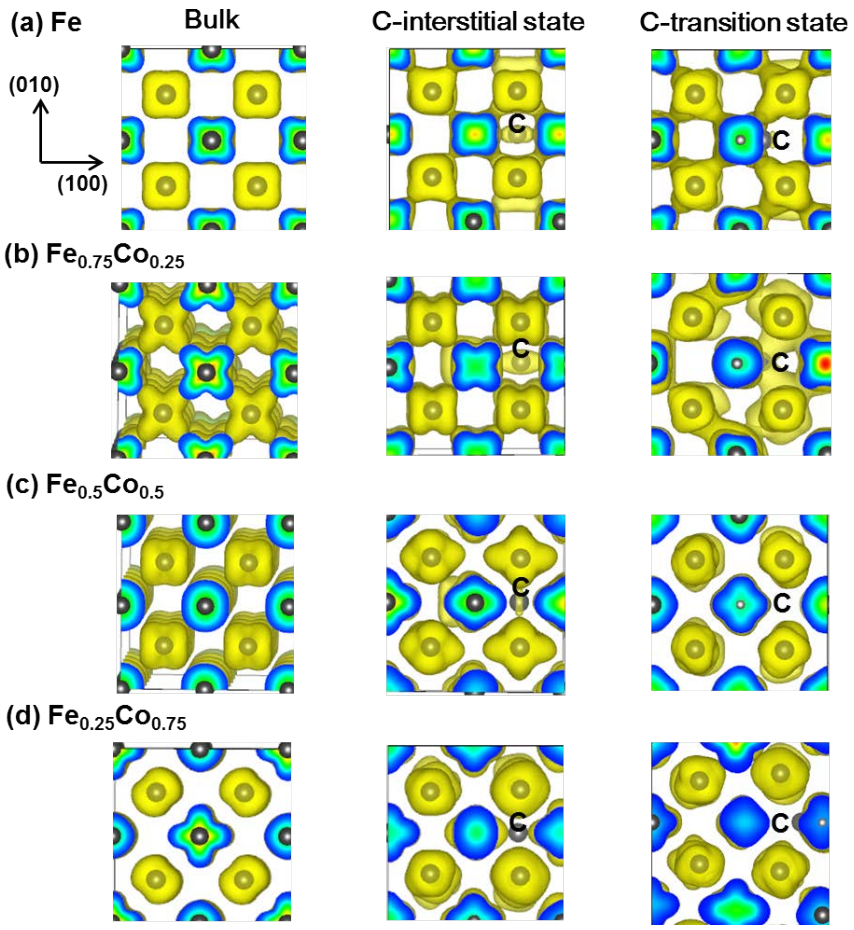


**Figure S11.** Calculated partial charge density of bulk, C-interstitial and C-transition state in (a) Fe, (b) $Fe_1Co_3$, (c) FeCo, and (d) $Fe_3Co_1$, respectively. The arrows indicate the surface direction and 'C' indicates the carbon atom.

| | Carbon ratio | Fe | $Fe_{0.75}Co_{0.25}$ | $Fe_{0.5}Co_{0.5}$ | $Fe_{0.25}Co_{0.75}$ |
|---|---|---|---|---|---|
| Carbon bulk formation energy | 0.78 % C (128 atoms) | 0.75 eV | 1.26 eV<br>1.27 eV<br>1.28 eV | 1.22 eV<br>1.87 eV | 0.58 eV<br>0.69 eV<br>1.43 eV |
| | 6.25 % C (16 atoms) | 0.91 eV | 1.36 eV<br>1.50 eV<br>1.53 eV | 1.65 eV<br>2.09 eV | 1.25 eV<br>1.30 eV<br>1.89 eV |
| Carbon bulk diffusion barrier | 0.78 % C (128 atoms) | 0.86 eV | 0.80 eV<br>0.74 eV<br>0.63 eV | 0.85 eV<br>0.21 eV | 0.85 eV<br>0.47 eV<br>0.40 eV |
| | 6.25 % C (16 atoms) | 0.85 eV | 0.65 eV<br>0.51 eV<br>0.55 eV | 0.58 eV<br>0.14 eV | 0.65 eV<br>0.28 eV<br>0.29 eV |

**Table S1.** Calculated dissolution energy and diffusion barrier of carbon for 0.78 % C and 6.25% C in Fe, $Fe_1Co_3$, FeCo, and $Fe_3Co_1$ . For 25% and 75% Co alloyed Fe, there are three possible stable energy configurations, and for 50% Co alloyed Fe, there are two possible stable energy configurations.

## References


1. Kresse, G. & Furthmuller, J. *Comp. Mater. Sci.* **1996**, 6, 15
2. Blochl, P. E. *Phys. Rev. B* **1994**, 50, 17953
3. Burke, K., Ernzerhof, M. & Perdew, J. P. *Chem. Phys. Lett.* **1997**, 265, 115
4. Nanda, K. K., Sahu, S. N. & Behera, S. N. *Phys. Rev. A* **2002**, 66, 013208